

Categorize Early, Integrate Late: Divergent Processing Strategies in Automatic Speech Recognition

Nathan Roll*, Pranav Bhalerao*, Martijn Bartelds, Arjun Pawar, Yuka Tatsumi, Tolulope Ogunremi, Chen Shani, Calbert Graham, Meghan Sumner, Dan Jurafsky

Stanford University

Abstract

In speech language modeling, two architectures dominate the frontier: the Transformer and the Conformer. However, it remains unknown whether their comparable performance stems from convergent processing strategies or distinct architectural inductive biases. We introduce *Architectural Fingerprinting*, a probing framework that isolates the effect of architecture on representation, and apply it to a controlled suite of 24 pre-trained encoders (39M–3.3B parameters). Our analysis reveals divergent hierarchies: Conformers implement a “Categorize Early” strategy, resolving phoneme categories 29% earlier in depth and speaker gender by 16% depth. In contrast, Transformers “Integrate Late,” deferring phoneme, accent, and duration encoding to deep layers (49–57%). These fingerprints suggest design heuristics: Conformers’ front-loaded categorization may benefit low-latency streaming, while Transformers’ deep integration may favor tasks requiring rich context and cross-utterance normalization.

1 Introduction

In text modeling, architectural diversity has largely collapsed onto the Transformer paradigm. Speech is different: two encoder families, Transformers and Conformers, coexist at the frontier, achieving comparable word error rates (WER) on standard benchmarks (Gulati et al., 2020; Radford et al., 2023). This coexistence creates a unique scientific opportunity. Unlike text, where representational convergence cannot be disentangled from architectural uniformity, speech allows us to ask: **when two architectures solve the same problem equally well, do they converge on similar internal processing strategies, or does architectural inductive bias produce fundamentally different solutions?**

*Equal contribution.

This question matters for three reasons. First, **interpretability**: knowing where phonetic and speaker information emerges enables targeted debugging and trust calibration. Second, **demographic encoding**: understanding when gender and accent cues become accessible informs fairness audits. Third, **deployment**: if architectures process information at different depths, this has implications for streaming, latency, and layer-wise pruning.

Prior probing work has established that speech models encode acoustic and linguistic information hierarchically (Belinkov et al., 2019; Pasad et al., 2021; Martin et al., 2023; Pasad et al., 2023), with phonetic information peaking in middle layers and word identity emerging later (Pasad et al., 2021; Bartelds et al., 2022). Complementary analyses have revealed speaker-specific and L1-related structure (Ferragne et al., 2019; Graham, 2021). However, no prior work systematically compares Transformer versus Conformer encoders to isolate how architectural inductive bias (rather than scale or training data) shapes representational hierarchies.

Our main contributions are:

1. We introduce *Architectural Fingerprinting*, a probing framework using linear probes to quantify when features become linearly accessible across depth, characterizing how architectural inductive bias shapes representational hierarchies. Our probes measure linear accessibility rather than making causal claims about mechanism.
2. We present a comprehensive, architecture-controlled analysis of 24 Transformer and Conformer models, revealing consistent, architecture-dependent representational profiles that persist across scale, dataset, and training regime despite comparable automatic speech recognition (ASR) performance.

3. We identify two divergent processing strategies: Conformers’ *Categorize Early* strategy, which front-loads phoneme category and gender information, versus Transformers’ *Integrate Late* strategy, which co-locates phoneme, accent, and duration cues in deeper layers (Figure 1).
4. We show that a logistic regression classifier predicts architecture from peak position profiles alone ($AUC = 0.88$), demonstrating that representational profiles are architecturally distinctive.
5. Code and data will be released upon publication to enable reproducibility and extension of our architectural fingerprinting framework.

2 Methods

Using linear probing (§2.3), we analyze 24 Transformer and Conformer models (§2.1) across over 50,000 utterances from seven speech corpora (§2.2). We extract layer-wise representations using standardized depth indexing (§2.4), quantify information accessibility with complementary metrics (§2.5), and apply statistical tests (§2.6) to isolate architectural effects while controlling for model scale. This approach reveals systematic differences in how architectures organize acoustic, demographic, phonetic, and temporal information.

2.1 Model Suite

We analyzed a diverse collection of 24 pre-trained spoken language models spanning two dominant speech encoder architectural families: Transformers (N=17) and Conformers (N=7). This imbalance reflects the current landscape of publicly available pretrained models and we address its statistical implications in §2.6. The models ranged in size from approximately 39M to 3.3B parameters, providing broad coverage across scales and training regimes. A complete list of all models is provided in Appendix A. All models were analyzed in their publicly released, pre-trained state without fine-tuning.

2.2 Dataset and Speech Corpora

For robustness, we probed model representations using seven diverse speech corpora spanning native and non-native English speakers, multiple accent backgrounds, and varied recording conditions: **L2-ARCTIC** (non-native English; Zhao et al., 2018); **CMU ARCTIC** (native English; Kominek and

Black, 2004); **Common Voice** (accent-stratified crowdsourced; Ardila et al., 2020); **Speech Accent Archive (SAA)** (elicited passage, 100+ L1s; Weinberger, 2015); **ALLSSTAR** (L2 acquisition research; Bradlow et al., 2010); **Cambridge Assessment** (proficiency assessment; Nicholls et al., 2022) and **SANDI** (clinical speech samples; Bergelson et al., 2017).

Our corpus comprises 50,000+ utterances across all datasets. Speech samples were processed at each model’s native sampling rate (typically 16 kHz) and segmented to match the temporal resolution required for phoneme-level analysis. Results were aggregated across datasets to ensure findings generalize beyond any single corpus. Detailed per-dataset statistics (size, sampling rate, segmentation) are provided in Table 4.

2.3 Feature Taxonomy and Probing

All analyses in this paper measure *linear accessibility* of information across network depth. Linear probes quantify when a feature can be extracted by a simple readout without additional nonlinear computation. This choice is intentional: linear accessibility reflects functional availability to downstream components and is the standard lens through which representational hierarchies are compared across architectures. We do not claim that linear probes exhaustively measure all information present in a representation; rather, our claims concern when information becomes linearly usable as depth increases.

Following the signal-to-symbol hierarchy established in speech perception research (Hickok and Poeppel, 2007; Poeppel et al., 2008) and validated in neural probing studies (Belinkov and Glass, 2017; Pasad et al., 2021), we organized features into four levels of abstraction: **Acoustic** (F0, formants, intensity), **Demographic** (gender, L1 accent), **Phonetic** (phoneme category), and **Temporal** (phoneme duration). We probe phoneme categories as defined by the CMU pronouncing dictionary (39 categories), which groups allophones of the same phoneme; our probes thus measure categorical sound identity rather than fine-grained allophonic variation. Detailed definitions for each feature are provided in Appendix E. For each model and layer, we trained linear probes to predict these features from hidden states (linear regression for continuous targets; logistic regression for categorical ones). Accordingly, probe curves should be interpreted as measuring *linear accessibility* rather

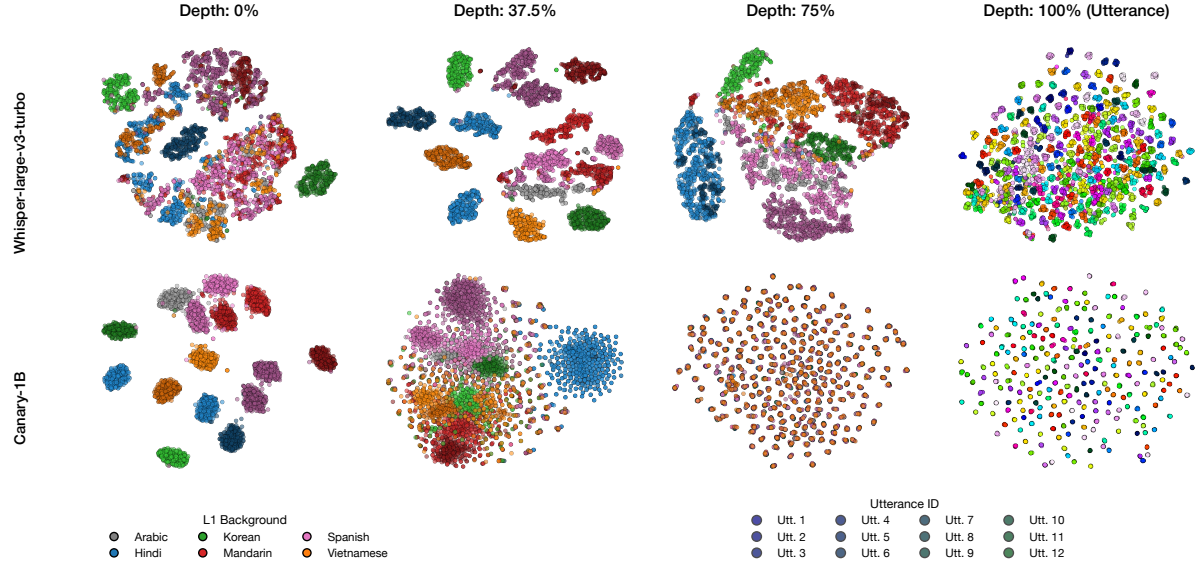


Figure 1: t-SNE visualization of encoder representations comparing a Transformer (Whisper-large-v3-turbo, top row) and a Conformer (Canary-1B, bottom row) across network depth. Each column shows representations at increasing depths (0%, 37.5%, 75%, and 100% of total layers). The first three columns are colored by L1 background: Arabic (gray), Hindi (blue), Korean (green), Mandarin (red), Spanish (magenta), and Vietnamese (orange). The rightmost column (100% depth) uses a distinct color palette, colored by utterance identity (12 discrete colors for 12 different utterances), to reveal how content clusters in the final layer independent of L1 background. Utterance colors are assigned arbitrarily and do not correspond to specific L1 backgrounds. Points are plotted in random order within each depth column to avoid visual occlusion bias. The Transformer shows gradual emergence of accent clustering in deep layers, while the Conformer exhibits earlier and sharper accent separation, consistent with their divergent processing hierarchies.

than raw information availability.

2.4 Depth Standardization

To standardize depth across heterogeneous ASR frontends, we extract the sequence of hidden states output by each encoder block. This yields $L + 1$ representations (an initial pre-block representation plus one per encoder block). Throughout, **Layer 0** denotes the *pre-block* encoder representation (i.e., the embedding/projection output immediately before the first encoder block), and Layer L denotes the final encoder block output. Importantly, this convention **does not treat convolutional feature-extractor frontends as additional layers**: when present, the feature encoder is upstream of the probed hidden-state stack and is not separately indexed. This ensures comparisons focus on the encoder depth where architectural differences (e.g., per-block convolution vs. attention-only blocks) are expressed. Implementation details for extracting these states across libraries are provided in Appendix A.5.

Stem compression caveat. Models with strong convolutional frontends (e.g., wav2vec2, Whisper) may already extract local patterns before Layer 0.

If Transformers perform early categorization in the stem, our probes would not detect it.

2.5 Evaluation Metrics

We evaluated probing performance using three complementary metrics, with formal definitions provided in Appendix C.

- **Peak Position (π_f):** The normalized network depth (0-1) where probe performance is maximized.
- **Peak Strength (s_f):** The maximum accuracy or R^2 achieved across all layers.
- **Positional Deltas ($\Delta\pi$):** The difference in peak position between two features or architectures.

2.6 Statistical Analysis

Architectural Comparison. To test whether peak positions differ systematically between architectures, we conducted two-sample t-tests comparing Transformer (N=17) and Conformer (N=7) models for each feature type. We report bootstrap 95% confidence intervals (10,000 resamples) for the mean difference in peak position.

Regression Analysis. To isolate the effect of architecture while controlling for model size, we fit a linear regression model: $\pi_f = \beta_0 + \beta_1 \cdot \text{arch} + \beta_2 \cdot \log(\text{params}) + \epsilon$, where arch is a binary indicator (Conformer = 1, Transformer = 0) and params is the parameter count. We report standardized coefficients (β) and p -values from two-tailed tests.

Architectural Fingerprinting. To quantify the distinctiveness of architectural fingerprints, we trained a logistic regression classifier to predict architecture (Transformer vs. Conformer) from the 5-dimensional feature vector $[\pi_{\text{acoustic}}, \pi_{\text{gender}}, \pi_{\text{accent}}, \pi_{\text{phoneme}}, \pi_{\text{duration}}]$. We used leave-one-out cross-validation and report the area under the ROC curve (AUC) as our primary metric.

3 Results

Our analysis reveals **systematic, architecture-dependent processing strategies that persist across scale and training regime** in how Transformer and Conformer models organize speech information.

3.1 Divergent Processing Hierarchies

Transformer and Conformer models follow distinct orderings of feature representations. **Transformers implement an integrated processing strategy** ($\text{Acoustic} \rightarrow \text{Gender} \rightarrow \{\text{Phoneme} \approx \text{Duration} \approx \text{Accent}\}$), where high-level linguistic and sociolinguistic information co-locate in layers at 49–57% of total depth.

In contrast, **Conformers exhibit a segregated hierarchy** ($\text{Gender} \rightarrow \text{Phoneme} \rightarrow \text{Acoustic} \rightarrow \text{Accent} \rightarrow \text{Duration}$). Notably, Conformers exhibit representational profiles consistent with front-loading categorical features like gender (mean $\pi = 0.16$, i.e., 16% of network depth) and phoneme identity (mean $\pi = 0.21$) before resolving fine-grained acoustic details, while deferring temporal integration (duration) to the final layers. These hierarchies are consistent: 71% of Transformers (12/17) show co-located late peaks (Phoneme, Duration, and Accent all $> 35\%$ depth), and 86% of Conformers (6/7) show early categorization with late temporal integration (Gender and Phoneme $< 50\%$ depth; Duration $> 50\%$ depth). Exceptions are typically driven by unique training regimes (e.g., multilingual multitask training). Figure 2 summarizes these peak positions across all features, and Table 1 provides per-model details showing

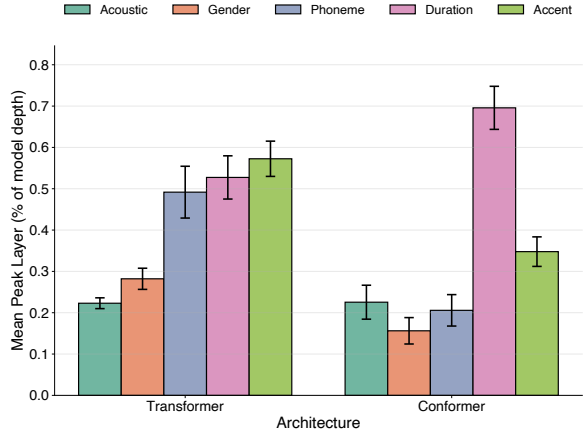


Figure 2: Mean peak layer position (as percentage of model depth) for five feature categories across Transformer (N=17) and Conformer (N=7) architectures. Error bars indicate standard error of the mean. The architectural divergence is clear: Conformers front-load Gender and Phoneme (both $< 25\%$ depth) while deferring Duration to final layers ($\sim 70\%$ depth), creating a distinct hierarchy. Transformers compress all high-level features into a narrow band (49–57% depth), reflecting their integrated processing strategy.

how individual models within each architectural family conform to these patterns.

3.2 Positional Dynamics of Individual Features

We examine how architectural inductive biases shape the encoding of specific features.

Acoustic features are front-loaded in both architectures (Transformer mean $\pi = 0.22$; Conformer mean $\pi = 0.23$), as expected for low-level signals.

Gender peaks very early in Conformers (mean $\pi = 0.16$), often *before* fine-grained acoustic features ($\pi = 0.23$), while Transformers distribute gender encoding more broadly (mean $\pi = 0.28$). Note that our use of binary gender labels reflects dataset annotations and may not capture the full spectrum of gender identity; similar caveats apply to coarse accent categories.

Phoneme category shows the largest divergence ($\Delta\pi = -0.29, p < 0.01$). Conformers peak early (mean $\pi = 0.21$) while Transformers peak late (mean $\pi = 0.49$).

Accent peaks earlier in Conformers (mean $\pi = 0.35$) than Transformers (mean $\pi = 0.57$).

Duration, requiring the longest-range integration, represents the final stage of processing for both architectures (Transformer $\pi = 0.53$; Conformer $\pi = 0.70$). We also found a universal hi-

Model	Acoustic	Gender	Accent	Phoneme	Duration
<i>Conformer Models</i>					
canary-1b	0.153	0.139	0.347	0.215	0.611
canary-1b-flash	0.146	0.089	0.260	0.130	0.849
canary-qwen-2.5b	0.151	0.099	0.255	0.312	0.464
granite-speech-3.3-2b	0.466	0.323	0.375	0.229	0.812
parakeet-tdt-0.6b-v2	0.194	0.167	0.340	0.340	0.611
speechbrain-loq	0.206	0.083	0.537	0.157	0.759
w2v2-conformer	0.192	0.194	0.319	0.056	0.764
<i>Transformer Models</i>					
Phi-4-multimodal	0.332	0.281	0.266	0.896	0.109
hubert-large	0.140	0.181	0.278	0.000	0.681
hubert-xlarge	0.091	0.073	0.271	0.156	0.538
wav2vec2-large	0.137	0.090	0.278	0.014	0.424
wavlm-large	0.186	0.118	0.618	0.500	0.667
whisper-base	0.306	0.333	0.722	0.472	0.472
whisper-base.en	0.258	0.278	0.667	0.778	0.472
whisper-large	0.217	0.297	0.698	0.245	0.552
whisper-large-v2	0.202	0.328	0.667	0.797	0.990
whisper-large-v3	0.202	0.406	0.708	0.604	1.000
whisper-large-v3-turbo	0.208	0.396	0.651	0.495	0.380
whisper-medium	0.172	0.292	0.618	0.417	0.465
whisper-medium.en	0.238	0.403	0.750	0.611	0.493
whisper-small	0.225	0.306	0.639	0.542	0.403
whisper-small.en	0.214	0.306	0.653	0.625	0.486
whisper-tiny	0.208	0.375	0.667	0.667	0.458
whisper-tiny.en	0.262	0.333	0.583	0.542	0.375

Table 1: Mean peak layer position for each model. Values represent the fraction of model depth (0 = first layer, 1 = final layer) where probing accuracy/R² is maximized. Conformers consistently show earlier Gender and Phoneme peaks compared to Transformers, while Duration peaks later in Conformers, reflecting their staged “Categorize Early” processing strategy.

erarchy in peak probing performance (Gender > Duration > Accent > Acoustic > Phoneme) across architectures; detailed results on representational entropy and outliers are provided in Appendix F.

Figure 3 visualizes these dynamics as smoothed probing trajectories across normalized depth. The Conformer curves show sharp early rises for Gender and Phoneme followed by plateau, while Transformer curves rise more gradually and peak in mid-to-deep layers. These trajectories underlie the summary statistics in Figure 2 and Table 1.

3.3 Architectural Fingerprints

The systematic differences we observe allow us to classify a model’s architecture from its representational profile alone with high accuracy (AUC = 0.88). The most discriminative features are accent ($\beta = -0.85$), gender ($\beta = -0.83$), and duration ($\beta = +0.81$). Controlling for model scale confirms these effects are architectural: **accent shows a significant architecture coefficient** ($\beta_{\text{arch}} = -0.21$, $p < 0.05$) independent of parameter count. Table 2 reports the complete statistical comparison, showing large effect sizes (Cohen’s $d > 0.8$) for all

Feature	$\Delta\pi$	t	df	p	Cohen’s d
Acoustic	+0.003	-0.08	22	0.940	0.03
Gender	-0.126	2.80	22	0.011	-1.26
Accent	-0.225	3.17	22	0.004	-1.42
Phoneme	-0.286	2.81	22	0.010	-1.26
Duration	+0.168	-1.90	22	0.071	0.85

Table 2: T-tests comparing peak positions between architectures. $\Delta\pi = \text{Conformer} - \text{Transformer}$ (negative values indicate Conformers peak earlier). Cohen’s $d > 0.8$ indicates large effect size. With Bonferroni correction for 5 comparisons ($\alpha = 0.01$), Accent and Phoneme survive correction.

features except Acoustic. With Bonferroni correction ($\alpha = 0.01$), Accent and Phoneme differences remain significant. Full statistical details including bootstrap confidence intervals are in Appendix B.

3.4 Architecture vs. Training Regime

While architecture explains most variance, training regime modulates specific features, as evident in the per-model peak positions shown in Table 1.

The “Whisper Effect”. Rather than treating Whisper as an anomaly, we interpret it as evidence for a

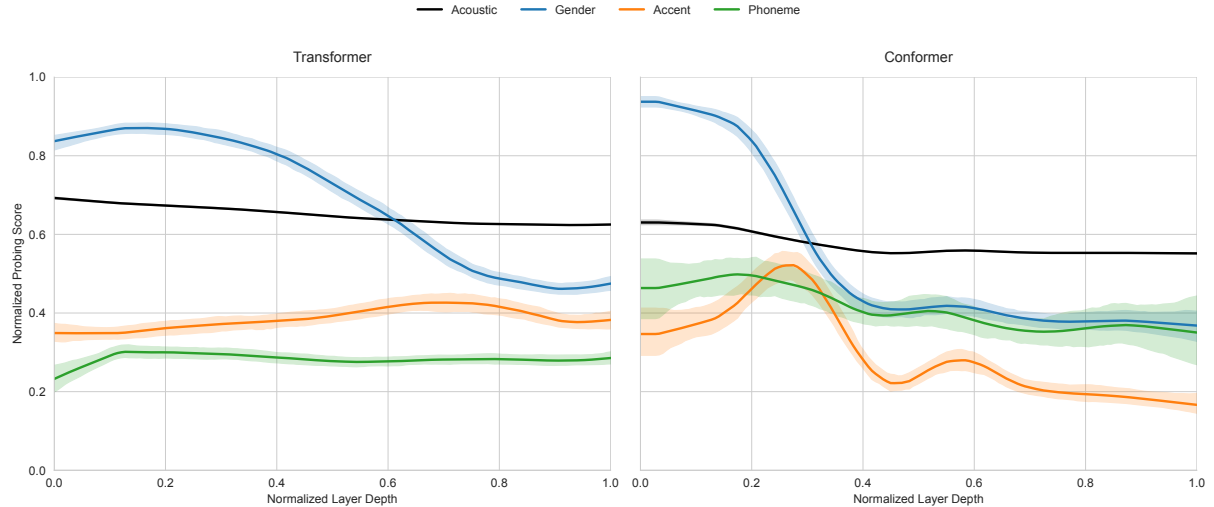


Figure 3: Smoothed layer-wise probing trajectories across normalized depth for representative feature groups (Acoustic, Gender, Accent, Phoneme), shown separately for Transformers (left) and Conformers (right). Curves are LOWESS fits with 95% bootstrapped confidence intervals. To emphasize *where* features become accessible (rather than absolute probe difficulty), probing scores within each feature group are min–max normalized before smoothing. Duration is omitted from this visualization for clarity; its peak positions are reported in Figure 2 and the main text.

hierarchy of controls: architecture sets the default representational profile, while objective acts as a modulator. Whisper models (supervised, multilingual) delay gender and accent processing significantly compared to SSL Transformers (HuBERT/WavLM), consistent with a multi-task objective that benefits from retaining indexical cues deeper in the network. However, the architectural fingerprint persists: non-Whisper Transformers still exhibit the “Integrate Late” strategy relative to Conformers (details in Appendix G).

3.5 Robustness and Controls

To ensure our findings are not driven by outliers or specific training factors, we conducted extensive robustness checks (detailed in Appendix D). A leave-one-out sensitivity analysis confirms that architectural effects become *stronger* when excluding the outlier model *granite-speech-3.3-2b* (e.g., gender $\Delta\pi$ improves from -0.13 to -0.15 , $p = 0.003$). Additionally, a paired comparison of multilingual vs. English-only Whisper models reveals no significant difference in peak positions for any feature (though phoneme shows a non-significant trend, $\Delta\pi = -0.12$, $p = 0.30$), indicating that the delayed processing in Whisper models is likely due to their multitask objective rather than multilingual data diversity.

4 Discussion

Our findings demonstrate that high-performance speech recognition emerges from fundamentally different processing strategies shaped by architectural inductive bias, not convergence to a single solution. The consistency of these architectural fingerprints, observable across model scales, training regimes, and even within sub-families, suggests we have uncovered organizing principles rather than superficial correlations. The ability to classify architecture from representational profiles alone ($AUC = 0.88$) underscores how inductive bias shapes the learned solution.

Comparison to Prior Work

Our findings extend prior probing work in three key ways. First, while past work established that self-supervised speech models encode features hierarchically (Pasad et al., 2021, 2023), they analyzed models individually without systematic architectural comparison. Our architecture-controlled analysis reveals that similar task performance can arise from fundamentally different processing strategies. Second, prior work focused primarily on *what* information is encoded (Belinkov and Glass, 2017; Sánchez et al., 2022), while we characterize *when* it becomes linearly accessible, enabling architectural fingerprinting. Third, the Conformer–Transformer divergence we document persists despite comparable ASR performance, echoing findings in NLP that

different architectures localize linguistic knowledge at different depths (Fayyaz et al., 2021). This demonstrates that benchmark parity does not imply representational convergence—a finding with implications for transfer learning, model selection, and interpretability.

Why Do These Divergent Strategies Emerge?

We propose that the observed differences arise from a distinction in how each architecture processes local versus global information.

Conformers’ “Categorize Early” Strategy. The Conformer’s depthwise separable convolutions may provide a strong inductive bias for local pattern detection. This is consistent with the rapid linear accessibility of categorical features (gender from coarse spectral patterns, phonemes from local acoustic templates) we observe in early layers. The staged pipeline, with 54% depth separation between gender and duration, suggests later layers perform higher-order integration.

Transformers’ “Integrate Late” Strategy. Pure self-attention lacks explicit local bias, which may require the network to learn local patterns implicitly through attention weights. This is consistent with the more gradual, distributed processing flow we observe. The co-location of accent, phoneme, and duration in the latter half of the network (all peaking between 49-57% depth) suggests these models resolve multiple feature types concurrently rather than through staged processing.

Objectives Modulate Architecture. The Whisper Effect (§3.4) demonstrates that training objectives can shift representational timing within an architectural family. This supports a “hierarchy of controls”: **architecture sets the default processing strategy; training objectives modulate it.** For practitioners, this suggests that architectural choice determines the *shape* of the representational profile, while objective choice fine-tunes *where* specific features peak. We emphasize that these are testable hypotheses grounded in linear accessibility patterns, not causal claims about mechanism.

Falsifiable Predictions

We offer falsifiable predictions for future work:

- **Nonlinear accessibility.** A shallow MLP probe could test whether early Transformer layers encode phoneme categories in a non-linearly separable geometry. Such a result would refine the interpretation from late integration

to late linearization, without affecting the finding that phoneme categories are not *linearly* accessible until deep layers in Transformers.

- **Within-block localization (Conformer).** If phoneme linear accessibility increases specifically after convolution sublayers (relative to attention sublayers) within Conformer blocks, this would implicate convolution modules as the driver of early categorization.
- **Hybrid encoders.** If hybrid architectures (e.g., E-Branchformer (Kim et al., 2023), Branchformer (Peng et al., 2022), Squeezeformer (Kim et al., 2022)) exhibit similarly early phoneme accessibility profiles, this would support the convolution-driven account; if not, the mechanism likely involves additional architectural interactions.

Implications for Model Design

Our findings suggest concrete selection heuristics:

- **Streaming and low-latency:** Conformers’ early phoneme category accessibility (21% depth vs. 49% for Transformers) means useful representations are available sooner. We predict Conformer-based systems will show smaller WER degradation under aggressive layer truncation or streaming constraints.
- **Speaker variability:** Transformers co-locate gender and accent with phoneme categories in deep layers, suggesting tighter integration of speaker normalization. We predict Transformer-based systems will show smaller performance gaps across speaker demographics when using full-depth representations. Recent work by Roll and Graham (2025) supports this hypothesis, finding that while Conformer-based models achieve lower overall WER, they exhibit substantially higher relative error rates on non-native speech (“conformation bias”) compared to Transformers.
- **Layer-wise distillation:** The staged Conformer hierarchy (gender → phoneme → acoustic → accent → duration) suggests natural cut-points for layer-wise knowledge distillation; the integrated Transformer profile may require different distillation strategies.

Future Directions. Hybrid architectures combining Conformer-style early convolutions with

Transformer-style deep integration capture benefits of both strategies, while training objectives may enable control over when features become accessible.

Limitations

Linearity vs. availability. Linear probes measure *linear accessibility* and cannot distinguish late *integration* from late *linearization*. Our claims are thus restricted to when information becomes linearly usable, not when it first emerges in any form. Testing nonlinear accessibility (as proposed in Falsifiable Predictions) would refine the interpretation of late accessibility without altering the architectural distinctions reported here.

Error pattern analysis. Our analysis characterizes *when* features emerge but not *how* they are represented. We cannot distinguish, for example, whether early Conformer phoneme encoding reflects local template matching or a different mechanism. Analyzing confusion matrices of phoneme probes could address this limitation, but such mechanistic validation is beyond our current scope.

Feature taxonomy scope. Our five-feature taxonomy captures the signal-to-phoneme transformation central to ASR but does not address lexical, syntactic, or discourse-level organization. Extending this to word-level semantics would provide a more complete picture of speech understanding.

Native vs. non-native speech. Our corpus includes both native speakers (CMU ARCTIC) and non-native speakers (L2-ARCTIC and others), but we do not systematically test for interactions between architecture and speaker nativeness. This limits our ability to characterize how architectural differences affect robustness to pronunciation variation, despite evidence that human listeners show processing delays for non-native accents (Munro and Derwing, 1995).

Model diversity. Our suite (24 models, 39M-3.3B parameters) does not include transducers (Graves, 2012) or state-space models, limiting generalization to the full ASR landscape.

Correlational nature. Our analysis is correlational: architecture predicts hierarchy, but cannot definitively establish causation. Controlled experiments (e.g., adding convolutions to Transformers) would provide stronger evidence but require training models from scratch, a substantial undertaking given the scale of modern ASR systems.

Ethical considerations. Our use of binary gender labels and coarse accent categories reflects dataset annotations but does not capture the full

spectrum of gender identity or accent diversity. Probing can expose sensitive attributes from representations, raising privacy concerns for deployment. We encourage practitioners to conduct fairness audits before using fingerprinting for model selection.

5 Conclusion

We demonstrated that state-of-the-art spoken language models do not converge on a single processing strategy; their **internal hierarchies are shaped by architectural inductive bias**. We identified two divergent pathways: a *segregated* “categorize early” hierarchy in Conformers, where gender and phoneme categories become linearly accessible in shallow layers before higher-order integration, and an *integrated, distributed* “integrate late” hierarchy in Transformers, which co-locates phoneme, accent, and duration cues in deeper layers.

These differences are quantifiable: phoneme category reaches its peak 29% earlier in Conformers than Transformers, representing the largest architectural effect we observed and surviving Bonferroni correction. In contrast, duration exhibits a trend toward later processing, peaking 17% deeper ($p = 0.071$). We show that a simple classifier can distinguish model families from representational profiles alone ($AUC = 0.88$, 95% CI [0.73, 1.00]), reinforcing the existence of stable architectural fingerprints (though the wide confidence interval reflects our moderate sample size).

Our findings reveal that high-performance speech recognition can emerge from different computational solutions. The path to expert performance is not singular: Conformers’ local-then-global inductive bias and Transformers’ global-only attention lead to different but equally effective processing strategies. This has practical implications for model selection (Conformers may excel at speaker-invariant tasks; Transformers at speaker-dependent ones) and underscores the impact of architectural priors on learned representations, paving the way for more intentional model design in speech processing. We envision Architectural Fingerprinting as a diagnostic tool for model developers: **a quick probe suite that reveals, before deployment, whether a model’s internal strategy matches the demands of the target task**.

References

Rosana Ardila, Megan Branson, Kelly Davis, Michael Henretty, Michael Kohler, Josh Meyer, Reuben

Morais, Lindsay Saunders, Francis M Tyers, and Gregor Weber. 2020. Common voice: A massively-multilingual speech corpus. In *Proceedings of the 12th Language Resources and Evaluation Conference*, pages 4211–4215.

Martijn Bartelds, Wietse de Vries, Faraz Sanal, Caitlin Richter, Mark Liberman, and Martijn Wieling. 2022. **Neural representations for modeling variation in speech.** *Journal of Phonetics*, 92:101137.

Yonatan Belinkov, Ahmed Ali, and James Glass. 2019. Analyzing phonetic and graphemic representations in end-to-end automatic speech recognition. In *Proc. Interspeech*, pages 81–85.

Yonatan Belinkov and James Glass. 2017. Analyzing hidden representations in end-to-end automatic speech recognition systems. In *Advances in Neural Information Processing Systems*, volume 30.

Elika Bergelson, Marisa Casillas, Melanie Soderstrom, Amanda Seidl, Anne S Warlaumont, and Andrei Amatuni. 2017. The sandi corpus: A structured collection of clinical speech samples. *Behavior Research Methods*, 49:2055–2065.

Paul Boersma and David Weenink. 2001. *Praat: doing phonetics by computer [Computer program]*. Version 6.0, retrieved from <http://www.praat.org/>.

Ann R Bradlow, David B Pisoni, Reiko Akahane-Yamada, and Yoh'ichi Tohkura. 2010. Allsstar: A structured list of standard sentences for tested articulation ratings. *Speech Communication*, 52(7-8):717–732.

Mohsen Fayyaz, Ehsan Aghazadeh, Ali Modarressi, Hossein Mohebbi, and Mohammad Taher Pilehvar. 2021. Not all models localize linguistic knowledge in the same place: A layer-wise probing on BERToids' representations. In *Proceedings of the Fourth BlackboxNLP Workshop on Analyzing and Interpreting Neural Networks for NLP*, pages 375–388.

Emmanuel Ferragne, Cédric Gendrot, and Thomas Pellegrini. 2019. Towards phonetic interpretability in deep learning applied to voice comparison. In *Proceedings of the International Congress of Phonetic Sciences (ICPhS)*, Melbourne, Australia.

Calbert Graham. 2021. L1 identification from l2 speech using neural spectrogram analysis. In *Proceedings of Interspeech*, pages 3959–3963.

Alex Graves. 2012. Sequence transduction with recurrent neural networks. In *International conference on machine learning*.

Anmol Gulati, James Qin, Chung-Cheng Chiu, Niki Parmar, Yu Zhang, Jiahui Yu, Wei Han, Shibo Wang, Zhengdong Zhang, Yonghui Wu, and Ruoming Pang. 2020. **Conformer: Convolution-augmented transformer for speech recognition.** In *Proceedings of Interspeech*, pages 5036–5040.

Gregory Hickok and David Poeppel. 2007. The cortical organization of speech processing. *Nature Reviews Neuroscience*, 8(5):393–402.

Kwangyoun Kim, Felix Wu, Yifan Peng, Jing Pan, Prashant Sridhar, Kyu J Han, and Shinji Watanabe. 2023. E-branchformer: Branchformer with enhanced merging for speech recognition. In *2022 IEEE Spoken Language Technology Workshop (SLT)*, pages 84–91. IEEE.

Sehoon Kim, Amir Gholami, Albert Shaw, Nicholas Lee, Karttikeya Mangber, Jitendra Malik, Michael W Mahoney, and Kurt Keutzer. 2022. Squeezeformer: An efficient transformer for automatic speech recognition. In *Advances in Neural Information Processing Systems*, volume 35, pages 9361–9373.

John Kominek and Alan W Black. 2004. The cmu arctic speech databases. *Fifth ISCA workshop on speech synthesis*.

Kinan Martin, Jon Gauthier, Canaan Breiss, and Roger Levy. 2023. Probing self-supervised speech models for phonetic and phonemic information: a case study in aspiration. In *Proc. Interspeech*.

Murray J Munro and Tracey M Derwing. 1995. Processing Time, Accent, and Comprehensibility in the Perception of Native and Foreign-Accented Speech. *Language and Speech*, 38(3):289–306.

Diane Nicholls, Ryan Sheridan, and Rogier van Dalen. 2022. Spoken language assessment using the cambridge assessment data. In *Proceedings of the 17th Workshop on Innovative Use of NLP for Building Educational Applications*, pages 189–198.

Ankita Pasad, Ju-Chieh Chou, and Karen Livescu. 2021. Layer-Wise Analysis of a Self-Supervised Speech Representation Models. In *2021 IEEE Automatic Speech Recognition and Understanding Workshop (ASRU)*, pages 914–921. IEEE.

Ankita Pasad, Bowen Shi, and Karen Livescu. 2023. Comparative Layer-Wise Analysis of Self-Supervised Speech Models. In *ICASSP 2023 - 2023 IEEE International Conference on Acoustics, Speech and Signal Processing (ICASSP)*, pages 1–5. IEEE.

Yifan Peng, Siddharth Dalmia, Ian Lane, and Shinji Watanabe. 2022. Branchformer: Parallel mlp-attention architectures to capture local and global context for speech recognition and understanding. In *International Conference on Machine Learning*, pages 17627–17643. PMLR.

David Poeppel, William J Idsardi, and Virginie Van Wassenhove. 2008. Speech perception at the interface of neurobiology and linguistics. *Philosophical Transactions of the Royal Society B: Biological Sciences*, 363(1493):1071–1086.

Alec Radford, Jong Wook Kim, Tao Xu, Greg Brockman, Christine McLeavey, and Ilya Sutskever. 2023.

Robust speech recognition via large-scale weak supervision. In *International Conference on Machine Learning*, pages 28492–28518. PMLR.

Nathan Roll and Calbert Graham. 2025. Scaling conformation bias in automatic speech recognition. In *Proc. SLATE*, pages 133–137.

Jorge Sánchez, Sameer Khurana, and James Glass. 2022. What does a self-supervised speech model hear? Layer-wise analysis of speech representations. In *Proc. Interspeech*, pages 4193–4197.

Steven H Weinberger. 2015. Speech accent archive. George Mason University. Retrieved from <http://accent.gmu.edu>.

Guanlong Zhao, Sabrina Sonsaat, Alif Silpachai, Ivana Lucic, Evgeny Chukharev-Hudilainen, John Levis, and Ricardo Gutierrez-Osuna. 2018. The l2-arctic corpus: A research resource for l2 pronunciation assessment and generation of speech. In *Proceedings of Interspeech*, pages 837–841.

A Experimental Details

A.1 Model Suite

Our analysis included 24 pre-trained models from the Transformer and Conformer families. Table 3 provides comprehensive architectural specifications.

A.2 Dataset Details

We aggregated probing results across seven speech corpora to ensure generalizability. Table 4 summarizes each dataset.

Results were computed per-dataset and then aggregated (mean peak positions across datasets) to ensure findings are not driven by idiosyncrasies of any single corpus. The L2-ARCTIC dataset (Zhao et al., 2018) was used for t-SNE visualizations (Figure 1) due to its balanced L1 representation.

A.3 Feature Extraction Details

A.3.1 Acoustic Features (24 probes)

Acoustic features were extracted using Praat (Boersma and Weenink, 2001) with a 10ms frame shift:

- **F0** (fundamental frequency): min, mean, median, max
- **F1, F2, F3** (formants): min, mean, median, max each
- **F3–F2** (formant dispersion): min, mean, median, max
- **Intensity**: min, mean, median, max

A.3.2 Demographic Features (2 probes)

- **Gender**: Binary classification (male/female).
- **L1 Background**: 6-way classification (Arabic, Hindi, Korean, Mandarin, Spanish, Vietnamese). We standardized L1 labels to these categories based on speaker metadata. For corpora with self-reported accent labels (e.g., Common Voice), we mapped to the nearest L1 category. Corpora without L1 metadata were excluded from accent probes.

For utterance-level labels (gender, accent), we applied the label to all frames within the utterance. Probes were trained at the frame level, but test accuracy was computed per-frame and then averaged per-utterance to avoid inflating sample sizes. We did not control for differences in frame stride across models, which is a limitation.

A.3.3 Linguistic Features (2 probes)

- **Phoneme category**: 39-way classification (CMU phoneme set, which groups allophones). Phoneme boundaries were obtained using the Montreal Forced Aligner (MFA) with the English pronunciation dictionary. For corpora lacking transcripts, we used Whisper-large-v3 for automatic transcription prior to alignment.
- **Duration**: Regression (phoneme duration in ms)

A.4 Linear Probe Training

Linear probes were trained independently for each feature at each layer:

- **Classification tasks**: Cross-entropy loss (Gender, L1, Phoneme)
- **Regression tasks**: Mean squared error loss (Acoustic, Duration)
- **Optimizer**: Adam with learning rate 0.001
- **Batch size**: 32
- **Max epochs**: 50 with early stopping
- **Data split**: 80%/10%/10% train/validation/test. For demographic probes (gender, accent), we used speaker-disjoint splits where possible (L2-ARCTIC, CMU ARCTIC). For corpora without speaker metadata, we applied random splits; this may inflate early-layer accuracy for these features, and we note this as a limitation.

Model	Arch	Params	Layers	Hidden	Heads	Training
<i>Transformer Models (N=17)</i>						
whisper-tiny	Trans.	39M	4	384	6	Supervised, 680k hrs
whisper-tiny.en	Trans.	39M	4	384	6	Supervised, English-only
whisper-base	Trans.	74M	6	512	8	Supervised, 680k hrs
whisper-base.en	Trans.	74M	6	512	8	Supervised, English-only
whisper-small	Trans.	244M	12	768	12	Supervised, 680k hrs
whisper-small.en	Trans.	244M	12	768	12	Supervised, English-only
whisper-medium	Trans.	769M	24	1024	16	Supervised, 680k hrs
whisper-medium.en	Trans.	769M	24	1024	16	Supervised, English-only
whisper-large	Trans.	1.55B	32	1280	20	Supervised, 680k hrs
whisper-large-v2	Trans.	1.55B	32	1280	20	Supervised, 680k hrs
whisper-large-v3	Trans.	1.55B	32	1280	20	Supervised, 1M+ hrs
whisper-large-v3-turbo	Trans.	809M	32	1280	20	Supervised, distilled
wav2vec2-large-960h-lv60	Trans.	317M	24	1024	16	SSL + fine-tuned
hubert-large-ls960-ft	Trans.	317M	24	1024	16	SSL + fine-tuned
hubert-xlarge-ls960-ft	Trans.	1B	48	1280	16	SSL + fine-tuned
wavlm-large	Trans.	317M	24	1024	16	SSL
Phi-4-multimodal-instruct	Trans.	2.7B	40	3072	32	Supervised, multimodal
<i>Conformer Models (N=7)</i>						
wav2vec2-conformer	Conf.	430M	24	1024	16	SSL
canary-1b	Conf.	1B	24	1024	8	Supervised, multilingual
canary-1b-flash	Conf.	1B	24	1024	8	Supervised, distilled
canary-qwen-2.5b	Conf.	2.5B	40	1536	12	Supervised, Qwen decoder
parakeet-tdt-0.6b-v2	Conf.	600M	30	768	8	Supervised, TDT
granite-speech-3.3-2b	Conf.	3.3B	32	2048	16	Supervised, code-switched
speechbrain-loq	Conf.	135M	12	512	8	Supervised

Table 3: Comprehensive model specifications. Trans. = Transformer, Conf. = Conformer. SSL = self-supervised learning. All Whisper models from OpenAI, HuBERT/Wav2Vec2 from Meta, WavLM from Microsoft, Canary/Parakeet from NVIDIA, Granite from IBM, SpeechBrain from community.

Dataset	Utterances	Rate (kHz)	Description	Segmentation
L2-ARCTIC	3,750	44.1	Non-native English, 6 L1s	MFA forced-aligned
CMU ARCTIC	4,500	16	Native English, regional accents	MFA forced-aligned
Common Voice	10,000+	48	Crowdsourced, accent-stratified	MFA forced-aligned
SAA	2,000+	44.1	Elicited passage, 100+ L1s	MFA forced-aligned
ALLSTAR	5,000+	44.1	L2 acquisition research	MFA forced-aligned
Cambridge	15,000+	16	Proficiency assessment	MFA forced-aligned
SANDI	3,000+	16	Clinical speech samples	MFA forced-aligned
Total	~50,000	–		

Table 4: Speech corpora used for probing. Utterance counts are approximate. All audio was resampled to 16 kHz for model inference. MFA = Montreal Forced Aligner.

A.5 Implementation Details

To extract hidden states consistently across models, we utilized the standard interface provided by the HuggingFace Transformers library. Specifically, models were invoked with `output_hidden_states=True`, returning a tuple containing the output of the embedding layer followed by the output of each Transformer or Conformer block. For models not in HuggingFace (e.g., some SpeechBrain or ESPnet models), we manually instrumented the forward pass to capture the equivalent intermediate representations.

B Detailed Statistical Results

B.1 Per-Model Peak Scores

Table 5 shows the maximum probing score achieved for each model across feature categories.

B.2 Complete Statistical Tests

B.2.1 Bootstrap Confidence Intervals

B.2.2 Regression Controlling for Model Size

B.3 Architectural Classifier Details

The logistic regression classifier for predicting architecture achieved:

- **AUC:** 0.88 (95% CI [0.73, 1.00])
- **Leave-one-out accuracy:** 19/24 = 79.2%

Standardized coefficients:

- Accent position: $\beta = -0.85$ (most discriminative)
- Gender position: $\beta = -0.83$
- Duration position: $\beta = +0.81$
- Acoustic position: $\beta = +0.68$
- Phoneme position: $\beta = -0.33$

Model	Acoustic	Gender	Accent	Phoneme	Duration
<i>Conformer Models</i>					
canary-1b	0.303	0.962	0.558	0.094	0.761
canary-1b-flash	0.305	0.960	0.574	0.079	0.834
canary-qwen-2.5b	0.302	0.959	0.557	0.107	0.748
granite-speech-3.3-2b	0.066	0.568	0.201	0.074	0.873
parakeet-tdt-0.6b-v2	0.307	0.951	0.554	0.079	0.727
speechbrain-loq	0.321	0.951	0.519	0.103	0.758
w2v2-conformer	0.311	0.962	0.461	0.168	0.786
<i>Transformer Models</i>					
Phi-4-multimodal	0.063	0.559	0.257	0.059	0.813
hubert-large	0.302	0.939	0.452	0.133	0.807
hubert-xlarge	0.302	0.938	0.466	0.102	0.823
wav2vec2-large	0.285	0.880	0.442	0.147	0.806
wavlm-large	0.276	0.883	0.514	0.118	0.785
whisper-base	0.308	0.952	0.467	0.083	0.913
whisper-base.en	0.301	0.917	0.464	0.082	0.901
whisper-large	0.339	0.943	0.592	0.095	0.917
whisper-large-v2	0.342	0.966	0.590	0.085	0.928
whisper-large-v3	0.343	0.959	0.582	0.063	0.929
whisper-large-v3-turbo	0.354	0.961	0.589	0.063	0.915
whisper-medium	0.337	0.952	0.587	0.088	0.900
whisper-medium.en	0.338	0.958	0.543	0.102	0.911
whisper-small	0.331	0.959	0.494	0.096	0.911
whisper-small.en	0.329	0.951	0.465	0.095	0.923
whisper-tiny	0.310	0.937	0.406	0.081	0.904
whisper-tiny.en	0.313	0.939	0.394	0.086	0.883

Table 5: Peak probing scores for each model. Acoustic/Duration values are R^2 ; Gender/Accent/Phoneme values are accuracy.

Feature	$\Delta\pi$	95% CI Low	95% CI High
Acoustic	+0.002	-0.061	+0.090
Gender	-0.126	-0.196	-0.046
Accent	-0.224	-0.321	-0.117
Phoneme	-0.286	-0.423	-0.146
Duration	+0.168	+0.029	+0.298

Table 6: Bootstrap 95% confidence intervals (10,000 resamples) for mean peak position differences between architectures.

Feature	β_{arch}	p_{arch}	β_{size}	p_{size}
Acoustic	+0.016	0.729	+0.004	0.803
Gender	-0.105	0.116	+0.002	0.908
Accent	-0.214	0.041	-0.024	0.425
Phoneme	-0.257	0.096	-0.006	0.901
Duration	+0.146	0.240	+0.042	0.276

Table 7: Linear regression: $\pi_f = \beta_0 + \beta_{\text{arch}} \cdot \text{Conformer} + \beta_{\text{size}} \cdot \log(\text{params})$.

B.4 Acoustic Feature Breakdown

Table 8 shows detailed statistics for individual acoustic features.

Feature	Transformer Pos	Conformer Pos	Score
F0 mean	0.167	0.662	0.067
F0 median	0.186	0.708	0.075
F0 min	0.286	0.179	0.283
F0 max	0.248	0.113	0.267
F1 mean	0.119	0.286	0.183
F1 median	0.138	0.283	0.200
F2 mean	0.154	0.280	0.170
F3 mean	0.138	0.362	0.114
F3 median	0.180	0.466	0.113
Intensity max	0.088	0.640	0.209
Intensity mean	0.152	0.532	0.154
			0.348
			0.376

Table 8: Selected acoustic feature positions and scores by architecture. Pos = mean peak layer position; Score = mean peak R^2 .

B.5 Whisper Model Family Analysis

C Formal Metric Definitions

C.0.1 Peak Position and Strength

For each feature f , we computed the **peak position** p_f as the normalized depth where probe performance was maximized:

$$p_f = \frac{\arg \max_l \text{score}_f(l)}{L}$$

where $\text{score}_f(l)$ is the test-set accuracy (for classification) or R^2 (for regression) at layer l , and L

Feature	Whisper	Non-Whisper	<i>p</i>
Gender	0.338	0.149	<0.001
Accent	0.669	0.342	<0.001
Duration	0.546	0.484	0.606

Table 9: Whisper (N=12) vs. non-Whisper Transformer (N=5) peak positions. Whisper models show significantly later gender and accent peaks.

is the total number of layers. Peak position ranges from 0 (first layer) to 1 (final layer). **Peak strength** s_f is defined as:

$$s_f = \max_l \text{score}_f(l)$$

C.0.2 Peak Width

To measure whether features are sharply localized or broadly distributed, we computed **peak width** w_f as the proportion of layers where performance exceeds 70% of peak strength:

$$w_f = \frac{1}{L+1} \sum_{l=0}^L \mathbb{1}[\text{score}_f(l) \geq 0.7 \cdot s_f]$$

Low values indicate sharp, localized peaks; high values indicate distributed encoding.

C.0.3 Positional Deltas

To quantify hierarchical separation between feature pairs, we computed **positional deltas**:

$$\Delta_{f_1 \rightarrow f_2} = p_{f_2} - p_{f_1}$$

Positive deltas indicate that feature f_2 peaks later than f_1 in the network.

C.0.4 Layer-wise Entropy

To measure the concentration of feature information, we computed the entropy of the normalized performance distribution across layers:

$$H_f = - \sum_{l=0}^L q_f(l) \log q_f(l)$$

where $q_f(l) = \frac{\text{score}_f(l)}{\sum_{l'} \text{score}_f(l')}$ is the normalized performance at layer l . High entropy indicates distributed encoding; low entropy indicates concentration in specific layers.

D Robustness Checks

D.1 Sensitivity Analysis: Robustness to Outliers

Given the small Conformer sample size (N=7) and the previously noted granite-speech-3.3-2b

anomaly, we conducted a leave-one-out sensitivity analysis to assess whether our conclusions depend on this outlier.

Excluding granite-speech: With N=6 Conformers, the architectural effects become *stronger*, not weaker:

- **Gender:** Δp changes from -0.126 to -0.154 ; p improves from 0.011 to 0.003, now surviving Bonferroni correction
- **Accent:** Δp remains stable at -0.23 ; $p = 0.007$
- **Phoneme:** Δp remains stable at -0.29 ; $p = 0.015$

This confirms that the “Categorize Early” hierarchy is a property of the Conformer architecture, not an artifact of the granite-speech outlier. Indeed, granite-speech’s late Gender peak (0.32 vs. Conformer mean 0.13) was *attenuating* the architectural effect.

D.2 Quantifying the Multilingual Effect

To isolate whether the “Whisper Anomaly” reflects multilingual training data rather than other factors, we performed a paired comparison of multilingual vs. English-only (.en) Whisper models at matched scales (tiny, base, small, medium; N=4 pairs).

Results: Surprisingly, multilingual training shows *no significant effect* on peak positions:

- Gender: $\Delta = -0.004$, $p = 0.93$ (no difference)
- Accent: $\Delta = -0.002$, $p = 0.97$ (no difference)
- Phoneme: $\Delta = -0.115$, $p = 0.30$ (trend, not significant)
- Duration: $\Delta = -0.007$, $p = 0.85$ (no difference)

Interpretation: The delayed gender and accent peaks in Whisper models are *not* attributable to multilingual vs. monolingual training data. Instead, the “Whisper effect” likely reflects other factors shared across all Whisper models: (1) the sheer scale of training data (680K+ hours), (2) the multi-task training objective (transcription + translation + language ID), or (3) architectural details specific to Whisper’s implementation. This finding refines our

earlier interpretation: the training *objective* (multitask) rather than training *data diversity* (multilingual) may be the key modulator of representational hierarchies.

E Feature Definitions

This appendix summarizes the feature taxonomy used for probing. Full dataset-specific extraction parameters, preprocessing, and label construction are included in Appendix A.

- **Acoustic:** F0, formants (F1–F3), intensity, and related summary statistics.
- **Demographic:** speaker gender (binary) and L1 background / accent (categorical).
- **Phonetic:** phoneme identity (categorical).
- **Temporal:** phoneme duration (continuous).

F Additional Results and Outliers

We provide expanded discussion of representational-strength trends, entropy/concentration summaries, and model-family heterogeneity. This includes additional detail on models that depart from canonical hierarchies and on objective-driven modulation (e.g., multitask training), complementing the main-text “hierarchy of controls” framing.

G Outliers and Training-Regime Analyses

Several models illustrate within-family heterogeneity without changing the primary Transformer-Conformer separation. For example, Whisper models delay gender and accent peaks relative to SSL Transformers, consistent with objective-driven modulation. We also observe a small number of outliers (e.g., multimodal Phi-4; hubert-large; granite-speech) with atypical peak patterns or reduced probe strength. We retain these models to avoid selective exclusion and report robustness checks in Appendix D.

H Reproducibility

All analyses were conducted using Python 3.9 with NumPy 2.0, SciPy 1.13, and scikit-learn 1.6. Probe training used PyTorch 2.0. Code for reproducing all analyses will be made publicly available upon publication. For the five architectural comparison

t-tests (one per feature), we applied Bonferroni correction, yielding a corrected significance threshold of $\alpha = 0.05/5 = 0.01$.

H.1 Software Versions

- Python 3.9
- NumPy 2.0.2
- Pandas 2.3.3
- SciPy 1.13.1
- Scikit-learn 1.6.1
- Statsmodels 0.14.6
- Matplotlib 3.9.2
- PyTorch 2.0

H.2 Computational Resources

Probing experiments were conducted on NVIDIA A100 GPUs. Each model’s full layer-wise probing (all features, all layers) required approximately 2–8 hours depending on model size.

H.3 Data Availability

The L2-ARCTIC dataset is publicly available. Model weights are available from HuggingFace Hub under their respective licenses (Apache 2.0 for most models). Code and probing results will be released upon publication.